HHS Public Access

Author manuscript

Cancer Res. Author manuscript; available in PMC 2018 October 28.

Published in final edited form as:

Cancer Res. 2017 November 01; 77(21): 5938–5951. doi:10.1158/0008-5472.CAN-17-1007.

Tethering IL2 to its receptor IL2Rβ enhances anti-tumor activity and expansion of natural killer NK92 cells

Youssef Jounaidi[1,*], **Joseph F. Cotten**[1], **Keith W. Miller**[1], and **Stuart A. Forman**[1]

[1]Department of Anesthesia, Critical Care and Pain Medicine, Massachusetts General Hospital and Harvard Medical School, 55 Fruit Street, Boston, MA 02114, USA

Abstract

Interleukin-2 (IL2) is an immunostimulatory cytokine for key immune cells including T cells and natural killer (NK) cells. Systemic IL2 supplementation could enhance NK-mediated immunity in a variety of diseases ranging from neoplasms to viral infection. However, its systemic use is restricted by its serious side effects and limited efficacy due to activation of T regulatory cells (Tregs). IL2 signaling is mediated through interactions with a multi-subunit receptor complex containing IL2Rα, IL2Rβ and IL2Rγ. Adult natural killer (NK) cells express only IL2Rβ and IL2Rγ subunits and are therefore relatively insensitive to IL2. To overcome these limitations, we created a novel chimeric IL2-IL2Rβ fusion protein of IL2 and its receptor IL2Rβ joined via a peptide linker (CIRB). NK92 cells expressing CIRB ($NK92^{CIRB}$) were highly activated and expanded indefinitely without exogenous IL2. When compared to an IL2-secreting NK92 cell line, $NK92^{CIRB}$ were more activated, cytotoxic and resistant to growth inhibition. Direct contact with cancer cells enhanced the cytotoxic character of $NK92^{CIRB}$ cells, which displayed superior in vivo antitumor effects in mice. Overall, our results showed how tethering IL2 to its receptor IL2Rβ eliminates the need for IL2Rα and IL2Rβ, offering a new tool to selectively activate and empower immune therapy.

Keywords

IL2 receptor; IL2; Natural killer cells; tumor; NK cells expansion; Cancer immunotherapy

INTRODUCTION

Natural killer (NK) cells are lymphocytes endowed with the innate ability to attack malignant and virus infected cells (1–3). Several interleukins, and in particular IL2, activate and expand T-cells and NK cells(4). Systemic IL2 supplementation could therefore enhance immunity in cancer and viral infection. However, tumor cells and their microenvironment (TME) often repress NK cells anti-tumor activity by orchestrating a multitude of escape mechanisms (5).

[*]To whom correspondence should be addressed Youssef Jounaidi Ph.D., Department of Anesthesia, Critical Care and Pain Medicine, Massachusetts General Hospital, 55 Fruit Street, Boston, MA 02114, USA, yjounaidi@mgh.harvard.edu.

Clinical trials using high dose IL2 infusions have met limited success due to severe side effects that mimic sepsis(6–8), while low-dose IL2 efficacy is limited by the short half-life (less than 10 min) of IL2 *in vivo*(9), and due to depletion of low IL2 doses by T-regs and other lymphoid cells(10). Several strategies based on IL2 have aimed to enhance NK cytotoxicity while reducing toxicity in patients, with limited efficacy. Cultured *ex-vivo* autologous NK cells activated and induced to proliferate by IL2 display less anti-tumor efficacy(11) than allogeneic NK cells (12), because self class I HLA signaling suppresses NK cytotoxicity and cytokine release(13). However, in order for allogeneic NK cells to be effective, pre-transfer lymphodepletion is required to reduce competition for growth factors and cytokines (14,15). Moreover, IL2 is needed to sustain NK cytotoxicity after *in vivo* transfer, exposing patients to systemic side effects.

Past efforts to express endogenous IL2 in NK cells (16) or to express membrane-bound endogenous IL2 (17) showed limited success with micro-metastatic models and were not as efficacious as NK cells stimulated with IL2 *ex-vivo*. The limited success of strategies using NK cells could be explained by the failure of activated NK cells to outcompete T-regs for cytokines in the host and the immunosuppressive effect of the TME, which includes myeloid derived suppressor cells (MDSCs). Both MDSCs and T-regs suppress NK cell functions either by direct contact or by secretion of TGFβ1(18,19).

To selectively activate and expand NK cells without exogenous IL2, while maintaining NK cytotoxicity and proliferation both *in vitro* and *in vivo*, circumvent the requirement of IL2Rα and its lack of expression in NK cells, thus avoiding IL2 off-target effects, cytokine competition, and activation of down-regulating lymphoid cells like T-regs. We created a novel chimeric IL2-IL2Rβ (CIRB), consisting of IL2 tethered *via* a linker to IL2Rβ, which functions like constitutively activated IL2Rβ. NK92 expressing CIRB ($NK92^{CIRB}$) produce anti-cancer effects *in vitro* that are equivalent to or better than $NK92^{IL2}$. Importantly, compared to IL2 stimulated NK92 and $NK92^{IL2}$, the anti-cancer activity and growth of $NK92^{CIRB}$ cells were resistant to the immunosuppressive cytokine TGFβ1 and dexamethasone. Moreover, the *in vivo* anti-cancer activity of $NK92^{CIRB}$ was significantly superior to that of $NK92^{IL2}$. $NK92^{CIRB}$ cells were also significantly more resistant to radiation and showed longer survival in tumor-bearing animals. Surprisingly, $NK92^{CIRB}$ and to a lesser extent $NK92^{IL2}$ express CD16, while it was not detected in IL2-stimulated NK92. CD16 expression synergized with Trastuzumab to exert substantial antibody dependent cellular cytotoxicity (ADCC). Additionally, $NK92^{CIRB}$ cells have higher expression of NKP30, NKP44 and Perforin-1 than $NK92^{IL2}$ and in contrast to $NK92^{IL2}$ increased their production of Granzyme-B, TNF-α and IFN-γ upon contact with cancer cells. In conclusion the novel chimera CIRB endows NK92 cells with very useful attributes that could improve immune therapy of cancer and potentially viral infections.

MATERIALS AND METHODS

Reagents

Dexamethasone (Dex), chloroquine, Matrigel (cat# 126–2.5) and human glycosylated IL2 (Sigma-Aldrich Co). Horse serum (HS), DMEM/F12, Lipofectamine 2000 and TRIzol (Life Technologies). Fetal bovine serum (FBS) (Atlanta Biologicals). RPMI 1640 (LONZA).

Smartscribe and Blueprint Onestep RT-PCR Takara kit (Clontech Laboratories); Platinum SYBR Green qPCR (Invitrogen), PfuUltra DNA polymerase (Stratagene). Human TGFβ1 (Antigenix America Inc). IL2 was from MGH-DF/HCC Recombinant Protein Core (Boston, MA). Human IL-4 (Shenandoah Biotechnology Inc). Anti-HER2 (Trastuzumab), humanized Antibody (BioVision Inc.) and PNGase F from New England Biolabs.

Cells

HEK293T, NK92, NK92-MI, PC-3, HepG2, MDA-MB-231, Panc-1, BT474 and U266 cells were from ATCC, U251GM a gift from Dr. Samuel Rabkin. U266-GFP-Luc cells were generated by lentiviral transduction using CSCW-GFP lentiviral vectors. Tumor cell lines PC-3, U251GM, U266, Panc-1, BT474 and MDA-MB-231 were cultured in complete RPMI1640 medium, HEK293T and HepG2 in complete DMEM/F12. NK92 and derived cell lines in RPMI1640 as described earlier (20) with 100 IU/ml IL2. All cell lines and assay cultures were maintained at 37°C and 5% CO2. All cell lines were obtained between 2015 and 2016 and were used until a maximum passage of 20 when they were replaced with a fresh passage. Monitoring for mycoplasma contamination was done using MycoFluor mycoplasma detection kit (Molecular Probes).

Chimera CIRB construction

IL2 cDNA was amplified from human brain total RNA by RT-PCR using Forward primer 5’-TGCAGGATCCACTCACAGTAACCTCAACTCC-3’ and reverse primer 5’-TGCACTCGAGAGTGAAACCATTTTAGAGCC-3’ and cloned in BamHI-XhoI in pCDNA4-TO. To build the CIRB chimera we first fused IL2 and the extracellular domain of its receptor IL2Rα, which was amplified by RT-PCR from NK92 total RNA using forward oligonucleotide 5’-GGATTACCTTTTGTCAAAGCATCATCTCAACACTGACTGAGCAGAAGCTCATTTCGGAAGAAGACCTTGAAATGGAGACCAGTCAGTTTCCAGG-3’, bridging IL2 C-terminal (12 amino acids before the stop codon), and contains the cMyc Tag, the sequence between amino acids 187–194 of IL2Rα as well as and the non-coding 3’ sequence of IL2 plasmid. This primer was used with reverse oligonucleotide 5’-CCTGATATGTTTTAAGTGGGAAGCACTTAATTATCAGATTGTTCTTCTACTC TTCCTCTGTCTCC −3’. The amplified fragment was used, as an oligonucleotide to mutagenize IL2 wild type resulting in an IL2-IL2Rα chimera. To build CIRB final chimera construct, the IL2-IL2Rα chimera was used to amplify IL2 with a C-terminal cMyc tag followed by only the extra cellular domain of IL2Rα then followed by the N-terminal fragment of IL2Rβ using Forward 5’-TGCAGGATCCACTCACAGTAACCTCAACTCC-3’ and reverse 5’-GGGAAGTGCCATTCACCGCGCAGGAAGTCTCACTCTCAGGA-3’. The product was then re-amplified using the same forward primer and the reverse 5’-GGCTCTCGAGTTGTAGAAGCATGTGAACTGGGAAGTGCC ATTCACCGC-3’. An XbaI site in IL2 was first removed by mutagenesis using primers forward 5’-CATCTTCAGTGCCTAGAAGAAGAACTC-3’ and reverse 5’-GAGTTCTTCTTCTAGGCACTGAAGATG-3’. IL2Rβ was then amplified using forward 5’-TTCCCAGTTCACATGCTTCTACAAGTCGACAGCCAACATCTCCTG-3’ and reverse 5’-AGCTTCTAGACTCGAGTTATCACACCAAGTGAGTTGGGTCCTGACCCTGG −3’. Next, the fragment

IL2-cMyc-IL2Rα was open Xho-XbaI and IL2Rβ was added as SalI-XbaI fragment to form the chimera CIRB. Both IL2 and CIRB were transferred from pcDNA4-TO using SpeI (blunt end) and XhoI to CSCW-mcherry digested with BamHI (blunt end) and XhoI. All constructs were sequenced..

Lentivirus production and NK cell lines transduction

HEK293T cells were transfected using Lipofectamine 2000 with 2.4 μg DNA of pVSV, (Clontech Laboratories), pCMVdr8.2dvrp Addgene (plasmid # 8455) and the lentiviral construct CSCW-GFP or CSCW-mCherry vectors MGH Vector Core (Boston, MA) to express either CIRB or IL2 constructs, using the ratios 1: 0.4: 1, respectively, with 25uM chloroquine. 6 hours post-transfection media was changed and lentiviral supernatant was collected 3 days later, filtered through a 0.45um syringe. NK92 cells were infected by spinoculation at 1800g for 45min at an optimal multiplicity of infection (MOI) of 46 lentiviral particles per cell in a 2ml-Eppendorf tube containing 2×10^5 cells. Infected cells were plated with IL2(100IU/ml) for two days, then weaned of exogenous IL2.

Western Blot

Phophorylated Stat 5 was detected using rabbit anti-STAT5 Phospho (Tyr694) antibody (BioLegend) while the chimera CIRB was detected by mouse anti-human IL2 antibody (Peprotech), in 40ug cell lysates obtained using Ripa lysis buffer (Santa Cruz Biotech). Secondary donkey anti-Mouse IRDye 800CW and goat anti-Rabbit IRDye 680RD antibodies were from Li-Cor, Biosciences.

Flow cytometry

NK cell markers expression was verified using mouse anti-human antibodies to CD45-APC-CY7, CD25-FITC, CD16-PE, CD3-PE-CY7, CD56-PAC BLUE and CD122-PE, were from BD Biosciences. Anti-human antibodies to NKG2D-APC, MHC-1 HLA-A2-APC, NKP30-PE, NKP44-PE-CY7, NKP46-FITC, Granzyme B-FITC, Perforin1-PE, Interferon-γ-APC, TNF-α1- APC-CY7, were from BioLegend, DAPI from Invitrogen, mouse anti-cMyc: sureLight APC was from Columbia Biosciences. Cells were sorted at MGH Flow Cytometry Core facility using a BD 5 laser SORP FACS Vantage SE Diva system (BD Biosciences). FACS data and ∑Median statistics were analyzed using FlowJo Software (Tree Star, Inc.). Human primary NK (hNK) cells were extracted from peripheral blood of healthy donors using the Rosettesep™ human enrichment kit (StemCell technologies).

Cytotoxic activity of NK92, $NK92^{IL2}$ and $NK92^{CIRB}$ cells

8×10^3 U266GFP cells (selected for firm adherence) were plated in triplicate in 96 well plates. 24 hours later $NK92^{IL2}$, $NK92^{CIRB}$ and NK92 (pre-stimulated for 24 hours with IL2, 100IU/ml) were added at effector/target cells ratios (E/T) of 1/8, 1/4, 1/2, 1/1 and 2/1. After two days of co-culture NK cells were suspended to allow further killing of U266GFP cells. After a total 4 days co-culture survival of U266GFP cells was quantified by GFP-emitted fluorescence.

In other experiments we evaluated NK cell lines anti-cancer effect against U251GM, PC-3, Panc-1, MDA-MB-231 and HepG2 cells. 32×10^3 cancer cells were first plated in a 24-well

plate for either 24 hours prior to adding NK92 (pre-stimulated with IL2, 100IU/ml), $NK92^{IL2}$ or $NK92^{CIRB}$ at E/T ratio of 2/1 target cancer cell, or only 5 hours before adding $NK92^{IL2}$ or $NK92^{CIRB}$ at E/T ratios of 0/1, 1/1, 2/1, and 3/1 for each cancer cell line. Co-cultured cells were then incubated for 4 days. Viability of cancer cells was determined using a 0.1% crystal violet in a10% alcohol solution followed by extraction using 70% ethanol and reading absorbance at 595nm.

ADCC of $NK92^{IL2}$ and $NK92^{CIRB}$ against HER2 positive breast cancer cell line

BT474 (8×10^3 cells) were plated in 96-well plates. 24 hours later cells were incubated for 20min at room temperature with 1ug/ml Trastuzumab before the addition of NK cells at an E/T ratio of 2:1. After 3 days of incubation, viability of cancer cells was determined using crystal violet staining.

Impact of pre-exposure to immunosuppressors on NK cells cytotoxicity and viability

NK92, NK92IL2 and NK92CIRB (64×103 cells), were plated and exposed for 24 hours to TGFβ1 (20ng/ml), or Dex (0.5uM). During this time NK92 cells were incubated with IL2 at 20IU/ml. U251GM, PC-3, Panc-1, MDA-MB-231 and HepG2 cells (32 ×103 cells) were then added to NK cells at an E/T ratio of 2:1. Co-cultured cells were incubated for 4 days and cell viability of cancer cells was determined using crystal violet staining.

To determine the impact of immunosuppressors TGFβ1, IL-4 and Dex on the growth of $NK92^{IL2}$ and $NK92^{CIRB}$ (30×10^3 cells), were plated in triplicate in a 12-well plate, grown under TGFβ1 (10ng/ml), IL-4 (10ng/ml), or Dex (1uM) for 3days, then refreshed for another 3 days of growth under the same conditions for a total of six days. Cells viability and growth were determined with Trypan blue exclusion using a Bio-Rad TC20™ automated cell counter.

Tumor Growth Delay Experiments

All experiments involving animals were approved by the IACUC at Massachusetts general Hospital. U251GM or PC-3 cells were suspended in serum-free RPMI1640 containing 20% Matrigel and injected sub-cutaneously (s.c.) as 4×10^6 cells for PC-3 or 3×10^6 cells for U251GM in a volume of 0.5 ml using a 0.5-inch 29-gauge needle and a 1 ml insulin syringe in week-old (24–25g) male NOD.Cg-Prkdcscid Il2rgtm1Wjl/SzJ immunodeficient mice (Jackson Laboratory). Tumor areas (length x width) were measured twice a week using Vernier calipers (Manostat Corp., Switzerland) and tumor volumes were calculated based on: Volume = $\pi/6$ (length x width)$^{3/2}$. Treatment with $NK92^{CIRB}$ or $NK92^{IL2}$ was initiated when the average tumor volume reached ~200 mm^3 for PC-3 or ~160mm^3 for U251. For animals bearing PC-3 tumors freshly prepared NK cells were suspended in PBS irradiated with 500cGy and administered as 4 weekly injections (15×10^6 cells in 200ul per mouse), via the tail vein. For animals bearing U251 cells $NK92^{CIRB}$ or $NK92^{IL2}$ were not irradiated.

Detection of $NK92^{CIRB}$ and $NK92^{IL2}$ in peripheral blood

U251MG tumor cells were grown s.c. in Nod/scid mice to ~160mm^3. Non-irradiated $NK92^{IL2}$ and $NK92^{CIRB}$ (10^7 cells), were injected, via the tail vein. A second injection of non-irradiated NK cells (5×10^6 cells) was carried out 4 days later. 17 days later, animals

were killed and cardiac blood was collected processed and analyzed by flow cytometry using human specific anti-CD45 and mCherry fluorescent protein.

Survival of irradiated NK92^{CIRB} and NK92^{IL2} cells-

After irradiation at 10Gy (0.83Gy for 12 min), NK92^{CIRB} and NK92^{IL2} were cultured and their survival was determined, using Trypan Blue exclusion every 24 hours for 3 days.

Expression profiles of cytotoxicity effectors in NK92, NK92^{IL2} and NK92^{CIRB}

Natural cytotoxicity receptors (NCRs): NKP30, NKP44, NKP46, cytolytic enzymes: Perforin-1 and Granzyme-B, and cytokines: TNFα and INFγ were quantified by qRT-PCR using the primers listed in supplementary Table S1. Protein expression profiles were also determined in NK cells by flow cytometry under TGFβ1 and dex treatments as well as under activation by contact with PC-3 cells

Statistical Analysis

Statistical significance of differences was determined by two-tailed Student's test, a one-way ANOVA, paired Tukey's Multiple Comparison test. All tests included comparisons to untreated samples or as indicated in the text. Statistical significance is indicated by *P<0.05, **P<0.01, ***P<0.001, ****P<0.001. Analyses were performed using Prism software version 6 (GraphPad Software).

Results:

Design and construction of the CIRB chimera

The quaternary crystal structure of IL2 receptors complex (21) shows that the C-terminal end of IL2 and the N-terminal residue of IL2Rβ are separated by 41Å. For a linker between IL2 and the N-terminus of IL2Rβ we choose the extracellular domain of IL2Rα. A cMyc tag was added between IL2 and the linker. The linker fold was predicted computationally to be a helix-dominated structure (supplementary Fig. S1). Linker flexibility was assessed using the computational method of Karplus and Shultz method (22) which, indicates better than average flexibility (1 or greater on a 0 to 2 scale) at all the peptide linkages. The mature receptor IL2Rβ protein without signal peptide was placed after the linker to yield the chimera CIRB. CIRB and IL2 were separately cloned in lentiviral vector co-expressing mCherry (Fig.1A).

Cell surface expression of the chimera CIRB

NK92^{IL2} and NK92^{CIRB} cell lines established with lentiviral infection at an identical MOI of 46, acquire IL2 independence and proliferate indefinitely. Both cell lines showed similar growth during a 6-days period, faster than NK92-MI another IL2-independent cell line (supplementary Fig. S2), with robust survival after subjection to multiple freezing and plating cycles in culture, comparatively to NK92 and NK92-MI. Using an anti-cMyc monoclonal antibody, we next examined the expression of CIRB at the cell surface of transiently transfected HEK293 (Fig. 1B) and stable NK92^{CIRB} (Fig. 1C). We found clear evidence of the surface expression of cMyc in NK92^{CIRB} but not in NK92^{IL2}. CIRB

expression was further confirmed using an anti-CD122 monoclonal antibody, which recognizes the native IL2Rβ as well as the chimera. Figure 1D shows the endogenous CD122 present in $NK92^{IL2}$ cells, as expected, but at levels lower than in $NK92^{CIRB}$, which express both IL2Rβ and CIRB. The expression of the full-length chimera CIRB was further detected by western blot using monoclonal anti-human IL2. Figure 1E shows a full-length size of 95 kDa, which is higher than the predicted size of 80kDa due to post-translational glycosylation. Indeed upon deglycosylation treatment with PNGase F, the chimera molecular weight was reduced to approximately 80Kda. Although IL2 produced by $NK92^{IL2}$ could be detected by RTPCR (Fig. 1F) and its secretion in the media could support the growth of bystander NK92 (Fig. 1G) it could not, however, be detected by western blot, as the limit of detection for anti-IL2 antibody is 3ng/lane. In fact the IL2-producing NK92-MI was reported to express 19.4 pg/ml an amount that could be detected only by Elisa (20).

Cytotoxicity of parental NK-92 and modified cell lines

We First compared cytotoxicity of NK92, $NK92^{IL2}$ and $NK92^{CIRB}$ cells against an adherent multiple myeloma cell line U266GFP. Figure 2A shows that NK92 cell line, although pre-stimulated with 100IU/ml of IL2, was far less cytotoxic than $NK92^{IL2}$ or $NK92^{CIRB}$. $NK92^{IL2}$ and $NK92^{CIRB}$ cells showed equivalent cytotoxicity toward U266GFP suggesting comparable levels of activation *in vitro*. NK92 cell line uniquely lacks killer immunoglobulin receptor (KIR). As a result, the cell surface expression of MHC-I in tumor cell lines should not account for a better or worse susceptibility to NK cell-mediated killing. We sought to confirm this for $NK92^{CIRB}$ by first determining the levels of the dominant MHC-1 antigen HLA-A2 in a panel of five human cancer cell lines. Figure 2B shows that, except for PC-3, the tumor cell lines we used in this study all express high HLA-A2 levels. We then compared anti-cancer activity of NK cell lines against five human cancer cell lines. In one experiment (Fig. 2C) cells were plated 24 hours prior to adding NK cell lines. At an E/T ratio of 2:1 the cytotoxicity of $NK92^{IL2}$ and $NK92^{CIRB}$ were generally equivalent with a slight edge to $NK92^{CIRB}$ and superior to NK92. In other experiments, cancer cells were plated only 5 hours prior to adding NK cells (Fig. 2D). Under these conditions, the cytotoxicity of all NK cell lines was greater than in cells plated for 24 hours. However, $NK92^{CIRB}$ showed more cytotoxicity than $NK92^{IL2}$, at most E/T ratios. This difference was more evident with the most resistant cancer cell lines U251GM and Panc-1. As expected, MHC-1 antigen HLA-A2 expression is irrelevant to $NK92^{CIRB}$ mediated cytotoxicity

$NK92^{CIRB}$ resistance to TGFβ1, IL4 and Dexamethasone immunosuppression

Transforming growth factor TGFβ1 is an immunosuppressor overexpressed in the TME, known to inhibit NK cells functions by destabilizing several activation signals (23). The glucocorticoid dexamethasone impairs the function of lymphocytes in part by suppressing IL2 production from CD4+ T cells (24). IL4 was reported to inhibit the proliferation of NK cells (25). We tested the effects of these immunosuppressors on $NK92^{IL2}$ and $NK92^{CIRB}$ by culturing cells for 6 days in the presence of TGFβ1 (10ng/ml), IL4 (10ng/ml), or dex (1uM). Figure 3A shows that $NK92^{IL2}$ did not survive the exposure to dex. Their proliferation was inhibited strongly by TGFβ1 and to some extent by IL4. In contrast, $NK92^{CIRB}$ proliferation was not significantly affected by TGFβ1 or IL4 and was weakly inhibited by dex (Fig. 3B).

The effects of TGFβ1 (20ng/ml), and dex (0.5uM) pre-treatments for 24hours on NK cell cytotoxicity were then evaluated against five cancer cell lines at an E/T ratio of 2:1 (Fig. 3C). NK cells affected more killing in these experimental conditions since cancer cells were added to already plated NK92 cells and are more vulnerable if not already attached. Additionally, NK92 cells were plated with IL2 in the media (20IU/ml) and are therefore more active than in other experiments. $NK92^{CIRB}$ cytotoxicity against MDA-MB-231, PC-3 and HepG2 was not affected. Dex severely reduced cytotoxicity of $NK92^{IL2}$ towards all cancer cell lines. Similarly, TGFβ1 significantly reduced $NK92^{IL2}$ cytotoxicity against most cancer cell lines except for MDA-MB-231 and HepG2. Surprisingly, NK92 cells also showed resistance to dex inhibition in MDA-MB-231 and HepG2, probably due to IL2 presence in the media. Overall immunosuppression of $NK92^{CIRB}$ was weaker than in the NK92 and $NK92^{IL2}$ lines and was also dependent on the target cancer cell line. Flow cytometry analysis shows both dex (1uM) and TGFβ1 (10ng/ml) affected NKP30 expression dramatically in $NK92^{IL2}$ (Fig. 3D), while $NK92^{CIRB}$ resisted dex and experienced a marginal effect under TGFβ1. NKP44 expression was equally but marginally reduced; while NKP46 was not affected in both cell lines. Annexin V staining shows that only dex induced moderate apoptosis in $NK92^{IL2}$ (11.5% cell death) while $NK92^{CIRB}$ apoptotic cells represented ~5 to 6%. Therefore, in $NK92^{IL2}$, the reduced cell growth under TGFβ1 and dex is probably caused by slow cell growth to which $NK92^{CIRB}$ cells are resistant.

CD16 is substantially induced by endogenous expression of the chimera CIRB

In accordance with their original characterization (26), NK92 cells were found $CD56^{+}$, $CD3^{-}$, $CD16^{-}$, $CD25^{+}$, $CD45^{+}$ and $NKg2D^{-}$ (Fig. 4A). $NK92^{CIRB}$ cells expressed higher amount of CD16 and lower amounts of CD25 than both IL2-stimulated NK92 and $NK92^{IL2}$. We also examined NK92-MI, and in accordance with a previous report (20), did not find any expression of CD16 (Fig. 4B). Similarly, CD16 was undetectable in NK92 treated with either glycosylated or non-glycosylated IL2 (Fig. 4C). Freshly isolated human NK (hNK) cells displayed different patterns of marker expression. Unlike NK92, the cell lines $NK92^{IL2}$, $NK92^{CIRB}$, and hNK cells are all $CD16^{+}$, with expression levels of hNK > $NK92^{CIRB}$ > $NK92^{IL2}$ (Fig. 4D). hNK cells express much higher levels of CD16 and NKG2D than all NK92 cell lines and are virtually CD25-negative. Of the NK92 cell lines, $NK92^{CIRB}$ expression for CD25 and CD16 were most similar to hNK.

ADCC of $NK92^{IL2}$ and $NK92^{CIRB}$ against HER2 positive breast cancer cell line BT474

We next examined the impact of CD16 expression on ADCC using Trastuzumab against an HER2 positive breast cancer cell line BT474. Figure 4E shows that in the absence Trastuzumab and when using an E/T ratio of 2:1, BT474 cells were not affected by the direct cytotoxicity of NK cells. However, in the presence of 1ug/ml Trastuzumab both $NK92^{CIRB}$ and $NK92^{IL2}$ exerted substantial cytotoxicity of about 60% and 50%, respectively. Trastuzumab alone at 1ug/ml did not affect significantly BT474 survival. Similarly NK92 did not provoke any significant cytotoxicity against BT474 in the presence of Tratstuzumab.

Activation and expression profiles of cytotoxicity effectors in NK92, $NK92^{IL2}$ and $NK92^{CIRB}$

Stat 5-phosphorylation, a downstream signaling associated with IL2 receptor activation was nearly identical between IL2-stimulated NK92 (100IU/ml) and $NK92^{CIRB}$ and modestly

higher by 17% in NK92^{IL2} suggesting an equivalency in activation signaling (Fig. 5A). However, qRT-PCR analysis (Fig. 5B) of NK92^{CIRB} revealed differences in the expression of NCRs: NKP30 (1.7 fold), NKP44 (9 fold) and NKP46 (1.4 fold), compared to NK92^{IL2} and NK92 stimulated with IL2 for 48 hours. In NK92^{IL2}, NKP44 expression also increased (3.3 fold). While Perforin-1 expression was similar in all cell lines, Granzyme-B expression declined and TNF-α increased in NK92^{IL2} and both declined marginally while INF-γ increased in NK92^{CIRB}. We sought to validate these data by investigating the protein expression of NK receptors (Fig. 5C) and effectors (Fig. 5D) by flow cytometry. A robust FlowJo statistic module revealed striking correlations between the RNA levels seen in Figure 5B and the histograms ∑median protein expression calculated in Figure 5E. To further delineate the major contributor(s) to NK cell lines cytotoxicity against cancer cells we determined the excess ratio of each protein between cell lines pairs. Figure 5F shows that NKP44 and NKP30 are the main differentiators between NK92^{IL2} and NK92 with an excess of 202% and 24% respectively. In NK92^{CIRB} this excess over NK92 is 303% and 61%. However, an excess of perforin-1 (21%) makes NK92^{CIRB} far more potent than NK92^{IL2}. Indeed a direct comparison of NK92^{IL2} and NK92^{CIRB} shows this latter to contain about 30% more of NKP30, 34% of NKP44 and 28% of Perforin-1. We also note that NKP30 expression was downregulated by dex and TGFβ1 in NK92^{IL2} rendering these cells less potent against cancer cells (Fig. 3D). Therefore, we deduce that NKP30, NKP44 and perforin-1 are distinguishing features of NK92^{CIRB} from NK92 and NK92^{IL2}.

In vivo detection of circulating NK92^{IL2} and NK92^{CIRB} cells

The Survival and systemic circulation of non-irradiated NK92^{IL2} and NK92^{CIRB} *in vivo*, were evaluated in the context of U251MG tumor-bearing animals. Figure 6A shows that within 24 hours of the first injection of live NK92^{CIRB} cells, rapid tumor volume regression of 46% was observed, while NK92^{IL2} cells caused 35% reduction. In contrast, tumors continued to grow in untreated animals to reach a maximal limit size nearing 200mm^3 before regressing. This size-dependent limited growth is due to the poor angiogenesis of these tumors, which can be improved by VEGF expression (27). Tumor regression for NK92^{CIRB}-treated group continued after the second injection while the tumors in NK92^{IL2}-treated animals resumed growth and did not respond until day 18. Three weeks later, the untreated and NK92^{IL2} groups showed a similar tumor size. In comparison the NK92^{CIRB}-treated group displayed a significant tumor volume reduction of 86%. 17days post-NK cells injections; blood from mice was analyzed by flow cytometry for cells expressing mCherry, and human CD45. Figure 6B shows that only NK cells expressing CIRB but not IL2 can persist in tumor bearing animals.

Survival of irradiated NK92^{IL2} and NK92^{CIRB} cells

FDA requires NK92 cells irradiation between 5 and 10Gy prior to infusion to prevent proliferation. The irradiated NK92 cells viability declines dramatically within 2 days. NK92^{IL2} and NK92^{CIRB} were irradiated at 10Gy (0.83gy for 12 min) and then plated in complete NK92 media to determine their survival using Trypan Blue every 24 hours. Figure 6C shows that 24hours post-irradiation, 57% of NK92^{CIRB} and 45% of NK92^{IL2} cells survive. The survival advantage of NK92^{CIRB} was statistically significant at days 1 and 2 (*$P<0.05$).

Anti-tumor efficacy of irradiated NK92^{IL2} and NK92^{CIRB} cells

Androgen receptor and PSA negative PC-3 cells (28), form very aggressive tumors in Nod/Scid mice. When tumor volumes reached ~200 mm^3 (day 28), irradiated NK cells (500cGy) were administered as 4 weekly injections via the tail vein. Figure 6D shows that the growth of PC-3 tumors in the NK92^{CIRB}-treated group was slowed after the first injection. After the last NK92^{CIRB} injection, a significant tumor growth delay of about 17 days was recorded in the period between 1st and 4th NK92^{CIRB} injections (**P<0.01), comparatively to the untreated group. In contrast, the NK92^{IL2}-treated group tumors produced only a tumor delay of 7 days from the untreated tumors group (*P<0.05).

NK92^{CIRB} cells activation by direct contact with cancer cells

To better understand the events occurring during NK92^{CIRB} and NK92^{IL2} contact with cancer cells. NK cells were co-cultured with PC-3 cells for 3 hours, after which their expression profile for NKP30, NKP44, NKP46 (Fig. 7A), Perforin-1, Granzyme-B, TNF-α and IFN-γ (Fig. 7B), were compared to those in NK cells grown alone. A robust statistical analysis of histograms ∑Median expression using FlowJo software revealed striking differences in activation between NK92^{IL2} and NK92^{CIRB} (Fig. 7C, and supplementary Table S2). While both cell lines have within three hours discharged 17.5% of their Perforin-1 content into PC-3 cells, Granzyme-B, TNFα and IFN-γ, were reduced in NK92^{IL2}, suggesting release, while they increased in NK92^{CIRB} by 36%, 21% and 16%, respectively. Since NK92^{CIRB} released Perforin-1 and because Granzyme-B is co-delivered with Perforin-1(29), this increase suggests replenishment of these effectors, which are usually released within minutes of contact with cancer cells. NKP46 remained unchanged in NK92^{CIRB} while surface expression of NKP30 and NKP44 were dramatically reduced by 23% and 18%, respectively but only by 7% and 11% in NK92^{IL2}. This reduction in surface markers upon contact with cancer cells suggest receptors internalization that occur upon their activation by ligands on cancer cells. The overexpression of NKP30 and NKP44 on NK92^{CIRB} compared to NK92^{IL2} could drive a stronger activation that would explain Granzyme,-B, TNFα and INF-γ high levels compared to NK92^{IL2}. After 3 hours of contact with cancer cells, NK92^{CIRB} cells still harbored all receptors and effectors in excess over NK92^{IL2} (supplementary Table S2).

Discussion

IL2 can bind to receptor IL2Rα (CD25) with low affinity (30), or with an intermediary affinity to IL2Rβ (CD122) when associated with the common IL2Rγ chain (CD132) (31,32). However, this binding affinity is higher when all three receptors are combined (33). Adult NK cells may express only IL2Rβ and IL2Rγ subunits(34) and are, therefore, relatively insensitive to low doses of IL2, but acquire sensitivity upon IL2Rα expression(35). A recently developed IL2 “superkine” (36) that bypasses IL2Rα by binding directly and with high affinity to IL2Rβ produced better antitumor effects than wild type IL2 in mice. However, it still causes some form of pulmonary edema.

We created a novel chimera CIRB made of IL2 and its receptor IL2Rβ, joined by a peptide linker derived from the extracellular domain of IL2Rα. The linker was computationally

determined as reasonably flexible, without adversely affecting the chimera stability which is generally inversely correlated to flexibility(37). CIRB induces indefinite cell expansion and conferred an *in vitro* cytotoxicity similar or higher than that elicited by IL2 expression. *In vivo,* the anticancer activity of $NK92^{CIRB}$ against solid tumors was superior to that elicited by $NK92^{IL2}$. Additionally, CIRB confers, in contrast to IL2, substantial resilience to TGFβ1, dexamethasone and IL4. This advantage could be crucial in the TME where TGFβ1 is secreted by a variety of cells including cancer associated fibroblasts(38), and exists in a membrane bound form on T-regs to induce NK cells anergy(39), or by MDSCs to inhibit NKG2D expression, and IFN-γ production in NK cells(40). Cancer cells also regularly shed tumor-derived exosomes (TDEs) containing membrane bound TGFβ1 that down regulate NKG2D(41), and inhibit IL2 signaling(42). TGFβ1 mediates NK inhibition by an induced microRNA (miR)-183 which represses the co-activator/adapter DAP12 expression, thus destabilizing several activation signals in NK cells(23). CIRB expression in $NK92^{CIRB}$ cells also provides resistance to dex while $NK92^{IL2}$ cells growth was halted. Dex impairs the function of lymphocytes in part by suppressing IL2 production from CD4+ T cells, and reducing the activation receptors NKG2D and Nkp46 in NK cells (24). Glucocorticoid hormones can interfere with macrophage activation and antigen presentation, repress the transcription of several pro-inflammatory cytokines, chemokines, cell adhesion molecules and enzymes involved in the inflammatory response(43). The extreme sensitivity of $NK92^{IL2}$ to dex, could be explained by the reported destabilization of IL2 RNA(44), which could potentially occur in $NK92^{IL2}$ but not when IL2 is fused with IL2Rβ RNA as in $NK92^{CIRB}$.

CIRB and to a lesser degree the stable expression of IL2 allowed substantial CD16 expression in NK92. However, exogenous recombinant IL2 was not able to mediate such expression. Similarly, NK92-MI which produces and secretes IL2 was found deficient in CD16, as previously reported(20). When combined with Trastuzumab CD16 expression further enhanced $NK92^{CIRB}$ and $NK92^{IL2}$ cytotoxicity by ADCC. Interestingly, CD25 expression declined dramatically in $NK92^{CIRB}$ (Fig. 4A). This unique phenotype of substantial CD16 and low CD25 expression can synergize with the ADCC-mediated action of approved therapeutic antibodies. CIRB induced substantial RNA expression of NKP44 (9 fold), NKP46 (1.4 fold) and NKP30 (1.7 fold) as well as a modest but significant increase in INFγ. As expected, CIRB induced protein expression increase for NKP44 (4 fold) and NKP30 (1.6 fold). Finally, Perforin-1 expression increased slightly by 21% in $NK92^{CIRB}$.

Furthermore, upon contact with PC-3 cancer cells $NK92^{CIRB}$ cells experienced an increase in Granzyme-B, TNF-α and IFN-γ while NKP30, NKP44 and Perforin-1 contents decreased suggesting activation and internalization of these receptors with release of perforin-1. These features might explain the superior anti-cancer effect of $NK92^{CIRB}$ *in vivo*. We note that NKP30 was downregulated in $NK92^{IL2}$ treated with dex and TGFβ1 (Fig. 3D), which led to a reduced anticancer activity (Fig. 3C). This could suggest a prominent role for NKP30 in $NK92^{CIRB}$ where it is overexpressed and might offer resistance against the action of dex and TGFβ1.

Genetic modifications introducing CD16 in NK cells were shown to increase NK cell-mediated ADCC against multiple myeloma when combined with Elotuzumab(45). CD16

induction only in NK92^{CIRB} and NK92^{IL2} but not in NK92-MI or NK92 stimulated with IL2 could be explained by the persistent IL2 signaling that somehow translates into stronger activation and growth of NK92^{CIRB} and NK92^{IL2}. In fact the growths rates of both NK92^{CIRB} and NK92^{IL2} were 2-fold that of NK92-MI (supplementary Fig. S2). Another indication of higher activation of NK92^{CIRB} and NK92^{IL2} is the dramatic induction of NKP44, compared to NK92 stimulated with IL2 for 48 hours. Additionally, NK92^{CIRB} can proliferate in vivo far longer and also have a better survival after irradiation than NK92^{IL2} cells. They also surpass that of NK92-MI when exposed to similar conditions (20). *In vitro*, NK92^{IL2} cells secrete sufficient IL2 to sustain their activation and proliferation. In vivo, however, they may not be able to produce enough IL2 extracellular concentrations to sustain proliferation. This could be compounded by the competition for IL2 by T-regs and other immune cells in an immune competent animal.

Many encouraging advances have been achieved in NK cell-directed immunotherapy(46). However, the increasing demand for NK cells expansion *ex-vivo* requires both highly activated cells and reduced costs of cell expansion. Cellular immunotherapy using donor NK cells is an emerging field that could achieve significant anti-cancer effects, safely and without the risk of inducing graft-versus-host disease (GVHD). This safety feature as well as the off tumor/on target toxicity are currently hindering the success of CAR-T technology(47). Several NK cell lines (Khyg-1, NKL, NKG, NK-YS, YT, YTS and HANK-1 cells) are currently used in preclinical studies. However, only NK92 was extensively evaluated for its safety and efficacy in clinical settings(48,49). Unlike primary hNK cells, NK92 cells constitute a stable and homogenous population, amenable to genetic modification by lentiviruses, a gene transfer platform that has shown a good safety profile for lymphocytes(50). Our novel strategy of fusing interleukins to their receptors is a novel platform that can achieve a far better cytokine activation, with specificity, and without systemic toxicity or competition by other cellular components of the immune system. Self-activation of NK cells provides several distinguishing features such as resilience to TGFβ1 or glucocorticoid hormones, substantial expression of CD16, higher survival after irradiation and a superior antitumor activity *in vivo*. This new cytokine-cytokine receptor platform may be further improved to enhance NK cells anticancer and possibly antiviral activity.

Supplementary Material

Refer to Web version on PubMed Central for supplementary material.

Acknowledgment:

The authors wish to thank Dr. Rooma Desai of this laboratory for helpful comments and suggestions and Prof. Raje Nopoor from the Center for Multiple Myeloma, Massachusetts General Hospital Cancer Center for her very helpful advice and suggestions.

Supported in part by a DAPPCM Innovation Grant 226026 (Y. Jounaidi), NIH grant GM089745 (S.A. Forman), NIH grant GM058448 (K.W. Miller) and NIH Grant HL117871 (J.F. Cotten).

References

1. Caligiuri MA. Human natural killer cells. Blood 2008;112(3):461–9. [PubMed: 18650461]

2. Vidal SM, Khakoo SI, Biron CA. Natural killer cell responses during viral infections: flexibility and conditioning of innate immunity by experience. Curr Opin Virol 2011;1(6):497–512. [PubMed: 22180766]

3. Orr MT, Lanier LL. Natural killer cell education and tolerance. Cell 2010;142(6):847–56. [PubMed: 20850008]

4. Malek TR. The biology of interleukin-2. Annu Rev Immunol 2008;26:453–79. [PubMed: 18062768]

5. Dahlberg CI, Sarhan D, Chrobok M, Duru AD, Alici E. Natural Killer Cell-Based Therapies Targeting Cancer: Possible Strategies to Gain and Sustain Anti-Tumor Activity. Front Immunol 2015;6:605. [PubMed: 26648934]

6. Maas RA, Dullens HF, Den Otter W. Interleukin-2 in cancer treatment: disappointing or (still) promising? A review. Cancer Immunol Immunother 1993;36(3):141–8. [PubMed: 8439974]

7. Glauser FL, DeBlois G, Bechard D, Fowler AA, Merchant R, Fairman RP. Cardiopulmonary toxicity of adoptive immunotherapy. Am J Med Sci 1988;296(6):406–12. [PubMed: 3063115]

8. Ardizzoni A, Bonavia M, Viale M, Baldini E, Mereu C, Verna A, et al. Biologic and clinical effects of continuous infusion interleukin-2 in patients with non-small cell lung cancer. Cancer 1994;73(5): 1353–60. [PubMed: 8111701]

9. Donohue JH, Rosenberg SA. The fate of interleukin-2 after in vivo administration. J Immunol 1983;130(5):2203–8. [PubMed: 6601147]

10. Shevach EM. Regulatory T cells in autoimmmunity*. Annu Rev Immunol 2000;18:423–49. [PubMed: 10837065]

11. Parkhurst MR, Riley JP, Dudley ME, Rosenberg SA. Adoptive transfer of autologous natural killer cells leads to high levels of circulating natural killer cells but does not mediate tumor regression. Clin Cancer Res 2011;17(19):6287–97. [PubMed: 21844012]

12. Rubnitz JE, Inaba H, Ribeiro RC, Pounds S, Rooney B, Bell T, et al. NKAML: a pilot study to determine the safety and feasibility of haploidentical natural killer cell transplantation in childhood acute myeloid leukemia. J Clin Oncol 2010;28(6):955–9. [PubMed: 20085940]

13. Vales-Gomez M, Reyburn HT, Mandelboim M, Strominger JL. Kinetics of interaction of HLA-C ligands with natural killer cell inhibitory receptors. Immunity 1998;9(3):337–44. [PubMed: 9768753]

14. Miller JS, Soignier Y, Panoskaltsis-Mortari A, McNearney SA, Yun GH, Fautsch SK, et al. Successful adoptive transfer and in vivo expansion of human haploidentical NK cells in patients with cancer. Blood 2005;105(8):3051–7. [PubMed: 15632206]

15. Geller MA, Cooley S, Judson PL, Ghebre R, Carson LF, Argenta PA, et al. A phase II study of allogeneic natural killer cell therapy to treat patients with recurrent ovarian and breast cancer. Cytotherapy 2011;13(1):98–107. [PubMed: 20849361]

16. Nagashima S, Mailliard R, Kashii Y, Reichert TE, Herberman RB, Robbins P, et al. Stable transduction of the interleukin-2 gene into human natural killer cell lines and their phenotypic and functional characterization in vitro and in vivo. Blood 1998;91(10):3850–61. [PubMed: 9573023]

17. Konstantinidis KV, Alici E, Aints A, Christensson B, Ljunggren HG, Dilber MS. Targeting IL-2 to the endoplasmic reticulum confines autocrine growth stimulation to NK-92 cells. Exp Hematol 2005;33(2):159–64. [PubMed: 15676209]

18. Mao Y, Sarhan D, Steven A, Seliger B, Kiessling R, Lundqvist A. Inhibition of tumor-derived prostaglandin-e2 blocks the induction of myeloid-derived suppressor cells and recovers natural killer cell activity. Clin Cancer Res 2014;20(15):4096–106. [PubMed: 24907113]

19. Bluestone JA, Abbas AK. Natural versus adaptive regulatory T cells. Nat Rev Immunol 2003;3(3): 253–7. [PubMed: 12658273]

20. Tam YK, Maki G, Miyagawa B, Hennemann B, Tonn T, Klingemann HG. Characterization of genetically altered, interleukin 2-independent natural killer cell lines suitable for adoptive cellular immunotherapy. Hum Gene Ther 1999;10(8):1359–73. [PubMed: 10365666]

21. Rickert M, Wang X, Boulanger MJ, Goriatcheva N, Garcia KC. The structure of interleukin-2 complexed with its alpha receptor. Science 2005;308(5727):1477–80. [PubMed: 15933202]

22. Vihinen M, Torkkila E, Riikonen P. Accuracy of protein flexibility predictions. Proteins 1994;19(2):141–9. [PubMed: 8090708]

23. Donatelli SS, Zhou JM, Gilvary DL, Eksioglu EA, Chen X, Cress WD, et al. TGF-beta-inducible microRNA-183 silences tumor-associated natural killer cells. Proc Natl Acad Sci U S A 2014;111(11):4203–8. [PubMed: 24586048]
24. Hsu AK, Quach H, Tai T, Prince HM, Harrison SJ, Trapani JA, et al. The immunostimulatory effect of lenalidomide on NK-cell function is profoundly inhibited by concurrent dexamethasone therapy. Blood 2011;117(5):1605–13. [PubMed: 20978269]
25. Nagler A, Lanier LL, Phillips JH. The effects of IL-4 on human natural killer cells. A potent regulator of IL-2 activation and proliferation. J Immunol 1988;141(7):2349–51. [PubMed: 3262658]
26. Gong JH, Maki G, Klingemann HG. Characterization of a human cell line (NK-92) with phenotypical and functional characteristics of activated natural killer cells. Leukemia 1994;8(4): 652–8. [PubMed: 8152260]
27. Ke LD, Shi YX, Yung WK. VEGF(121), VEGF(165) overexpression enhances tumorigenicity in U251 MG but not in NG-1 glioma cells. Cancer Res 2002;62(6):1854–61. [PubMed: 11912165]
28. Kaighn ME, Narayan KS, Ohnuki Y, Lechner JF, Jones LW. Establishment and characterization of a human prostatic carcinoma cell line (PC-3). Invest Urol 1979;17(1):16–23. [PubMed: 447482]
29. Lopez JA, Susanto O, Jenkins MR, Lukoyanova N, Sutton VR, Law RH, et al. Perforin forms transient pores on the target cell plasma membrane to facilitate rapid access of granzymes during killer cell attack. Blood 2013;121(14):2659–68. [PubMed: 23377437]
30. Leonard WJ, Depper JM, Crabtree GR, Rudikoff S, Pumphrey J, Robb RJ, et al. Molecular cloning and expression of cDNAs for the human interleukin-2 receptor. Nature 1984;311(5987):626–31. [PubMed: 6090948]
31. Hatakeyama M, Tsudo M, Minamoto S, Kono T, Doi T, Miyata T, et al. Interleukin-2 receptor beta chain gene: generation of three receptor forms by cloned human alpha and beta chain cDNA's. Science 1989;244(4904):551–6. [PubMed: 2785715]
32. Takeshita T, Asao H, Ohtani K, Ishii N, Kumaki S, Tanaka N, et al. Cloning of the gamma chain of the human IL-2 receptor. Science 1992;257(5068):379–82. [PubMed: 1631559]
33. Stauber DJ, Debler EW, Horton PA, Smith KA, Wilson IA. Crystal structure of the IL-2 signaling complex: paradigm for a heterotrimeric cytokine receptor. Proc Natl Acad Sci U S A 2006;103(8): 2788–93. [PubMed: 16477002]
34. Voss SD, Sondel PM, Robb RJ. Characterization of the interleukin 2 receptors (IL-2R) expressed on human natural killer cells activated in vivo by IL-2: association of the p64 IL-2R gamma chain with the IL-2R beta chain in functional intermediate-affinity IL-2R. J Exp Med 1992;176(2):531–41. [PubMed: 1500859]
35. Caligiuri MA, Zmuidzinas A, Manley TJ, Levine H, Smith KA, Ritz J. Functional consequences of interleukin 2 receptor expression on resting human lymphocytes. Identification of a novel natural killer cell subset with high affinity receptors. J Exp Med 1990;171(5):1509–26. [PubMed: 1692080]
36. Levin AM, Bates DL, Ring AM, Krieg C, Lin JT, Su L, et al. Exploiting a natural conformational switch to engineer an interleukin-2 'superkine'. Nature 2012;484(7395):529–33. [PubMed: 22446627]
37. Vihinen M Relationship of protein flexibility to thermostability. Protein Eng 1987;1(6):477–80. [PubMed: 3508295]
38. Lohr M, Schmidt C, Ringel J, Kluth M, Muller P, Nizze H, et al. Transforming growth factor-beta1 induces desmoplasia in an experimental model of human pancreatic carcinoma. Cancer Res 2001;61(2):550–5. [PubMed: 11212248]
39. Ghiringhelli F, Menard C, Terme M, Flament C, Taieb J, Chaput N, et al. CD4+CD25+ regulatory T cells inhibit natural killer cell functions in a transforming growth factor-beta-dependent manner. J Exp Med 2005;202(8):1075–85. [PubMed: 16230475]
40. Li H, Han Y, Guo Q, Zhang M, Cao X. Cancer-expanded myeloid-derived suppressor cells induce anergy of NK cells through membrane-bound TGF-beta 1. J Immunol 2009;182(1):240–9. [PubMed: 19109155]
41. Clayton A, Mitchell JP, Court J, Linnane S, Mason MD, Tabi Z. Human tumor-derived exosomes down-modulate NKG2D expression. J Immunol 2008;180(11):7249–58. [PubMed: 18490724]

42. Clayton A, Mitchell JP, Court J, Mason MD, Tabi Z. Human tumor-derived exosomes selectively impair lymphocyte responses to interleukin-2. Cancer Res 2007;67(15):7458–66. [PubMed: 17671216]

43. Barnes PJ. Anti-inflammatory actions of glucocorticoids: molecular mechanisms. Clin Sci (Lond) 1998;94(6):557–72. [PubMed: 9854452]

44. Boumpas DT, Anastassiou ED, Older SA, Tsokos GC, Nelson DL, Balow JE. Dexamethasone inhibits human interleukin 2 but not interleukin 2 receptor gene expression in vitro at the level of nuclear transcription. J Clin Invest 1991;87(5):1739–47. [PubMed: 2022743]

45. Tai YT, Dillon M, Song W, Leiba M, Li XF, Burger P, et al. Anti-CS1 humanized monoclonal antibody HuLuc63 inhibits myeloma cell adhesion and induces antibody-dependent cellular cytotoxicity in the bone marrow milieu. Blood 2008;112(4):1329–37. [PubMed: 17906076]

46. Terme M, Ullrich E, Delahaye NF, Chaput N, Zitvogel L. Natural killer cell-directed therapies: moving from unexpected results to successful strategies. Nat Immunol 2008;9(5):486–94. [PubMed: 18425105]

47. Glienke W, Esser R, Priesner C, Suerth JD, Schambach A, Wels WS, et al. Advantages and applications of CAR-expressing natural killer cells. Front Pharmacol 2015;6:21. [PubMed: 25729364]

48. Tonn T, Schwabe D, Klingemann HG, Becker S, Esser R, Koehl U, et al. Treatment of patients with advanced cancer with the natural killer cell line NK-92. Cytotherapy 2013;15(12):1563–70. [PubMed: 24094496]

49. Arai S, Meagher R, Swearingen M, Myint H, Rich E, Martinson J, et al. Infusion of the allogeneic cell line NK-92 in patients with advanced renal cell cancer or melanoma: a phase I trial. Cytotherapy 2008;10(6):625–32. [PubMed: 18836917]

50. Suerth JD, Schambach A, Baum C. Genetic modification of lymphocytes by retrovirus-based vectors. Curr Opin Immunol 2012;24(5):598–608. [PubMed: 22995202]

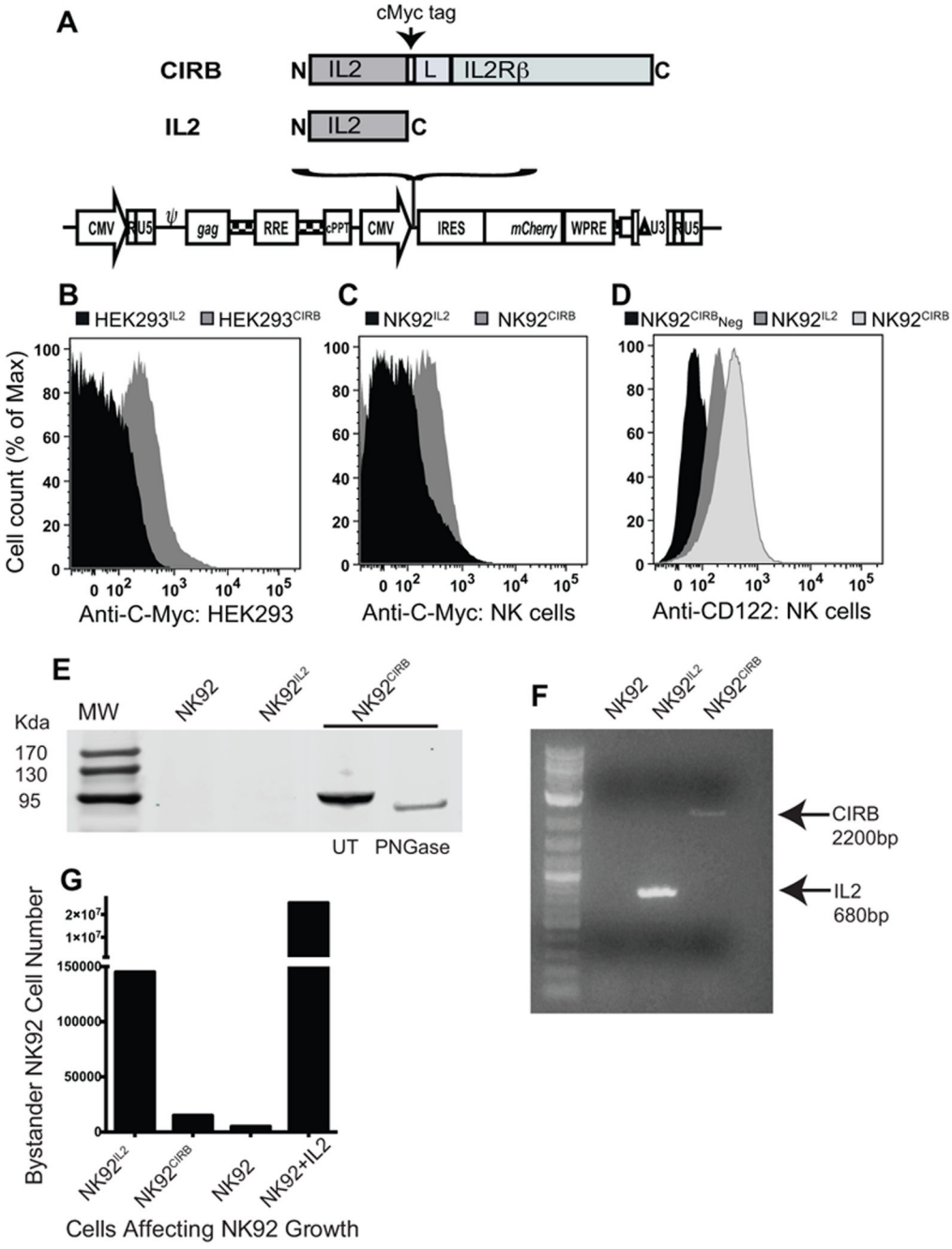

Figure 1.

CIRB a novel cytokine-cytokine receptor chimera **A**, Diagram of the Human IL2 and the chimera IL2 fused with receptor IL2Rβ (CIRB) in lentiviral constructs. A Linker (L) composed of the cMyc tag (EQKLISEEDL) and a fragment of the extracellular domain of IL2 receptor alpha (EMETSQFPGEEKPQASPEGRPESETSC), joins IL2 and its receptor IL2Rβ. **B**, detection by anti-cMyc monoclonal antibody of CIRB expression at the surface of transiently transfected HEK293 cells and **C,** in lentivirus transduced NK92 cells. **D**, CD122 expression detected using an anti-CD122 monoclonal antibody, which recognizes the native IL2Rβ (CD122) as well as the chimera. CD122 is present in $NK92^{IL2}$ cells and as expected,

much higher in $NK92^{CIRB}$ due to the additional expression of CIRB. Expression was higher than the background detected in the absence of antibody (Neg). **E**, CIRB was further detected by western blot using 40ug cell lysates and monoclonal anti-human IL2. CIRB is heavily glycosylated. **F**, RT-PCR detection of IL2 and CIRB transcripts in $NK92^{IL2}$ and $NK92^{CIRB}$. Primers sequences in Supplementary Table S1. **G,** Only $NK92^{IL2}$ cells secrete soluble IL2 that could support the growth of co-cultured NK92 cells. Experiment done in six-well plate with inserts containing 100K cells of bystander NK92 in the lower chamber and 100K cells of $NK92^{IL2}$, $NK92^{CIRB}$, NK92 or NK92 in the presence of IL2 (20IU/ml)

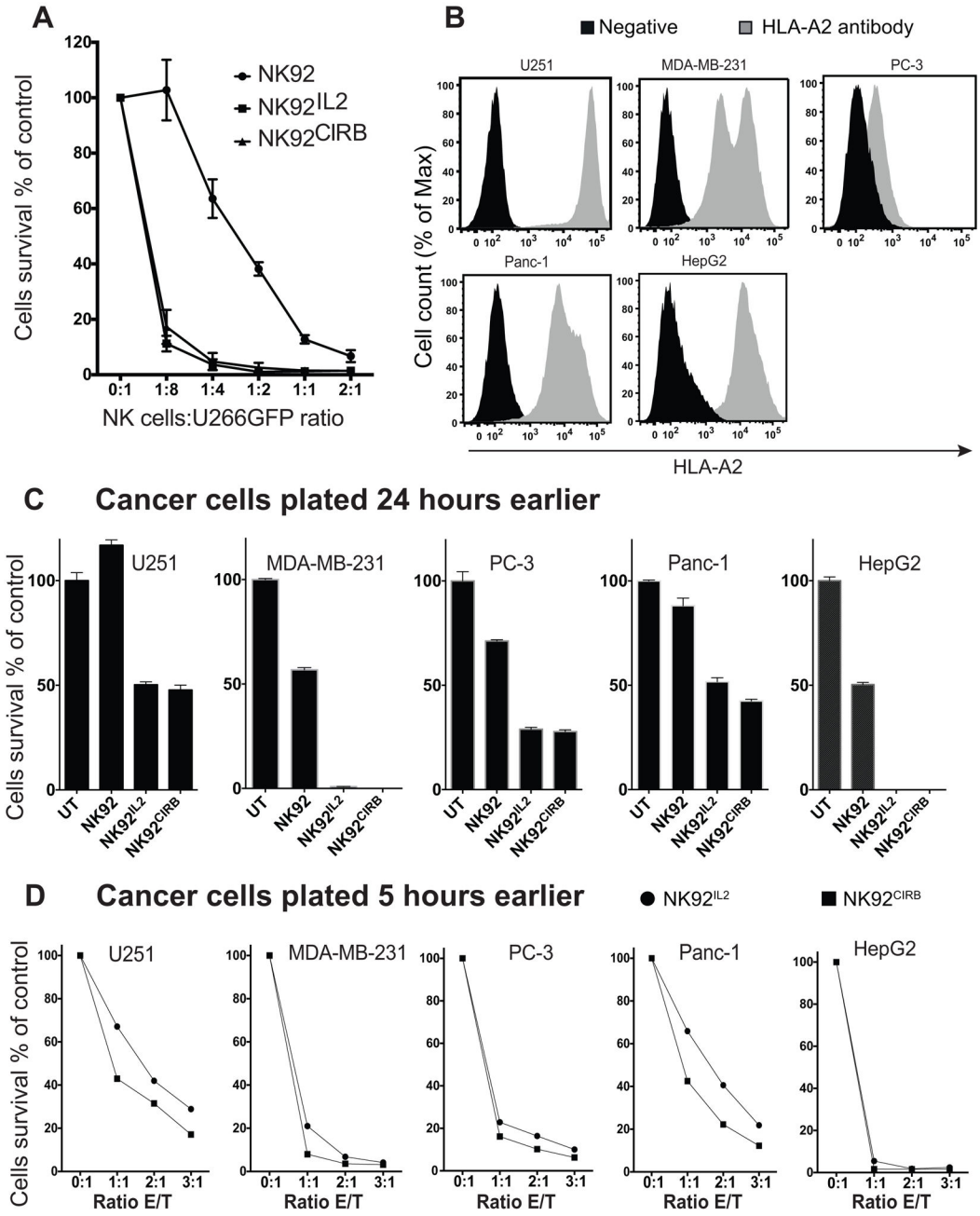

Figure 2.

Cytotoxicity of NK cell lines. **A**, cytotoxicity assays of NK92^{IL2}, NK92^{CIRB}, and NK92 cell lines against multiple myeloma U266GFP cells plated 24 hours prior to co-culture. Increased E/T ratios of NK cells induced more U266GFP cell death. U266GFP cell survival was evaluated using a SpectraMax® M2 fluorescence reader (Molecular Devices) with excitation at 485nm and emission at 515nm. **B**, Using anti-human HLA-A2-APC antibody flow cytometry shows the lack of correlation between the expression of HLA-A2 in all cancer cell lines used and their degree of sensitivity to NK92^{IL2} or NK92^{CIRB} reported in figure 3C. **C**, cytotoxicity assay against a panel of five human cancer cell lines: U251GM, PC-3, Panc-1,

MDA-MB-231 and HepG2 cells. Cells were plated 24 hours prior to adding NK cell lines at E/T ratio of 2:1. While in **D,** cancer cells were plated only 5 hours prior to exposure to increasing E/T ratios of $NK92^{IL2}$ (), or $NK92^{CIRB}$ () cells. Remaining cells after this time were determined using a crystal violet/alcohol-extraction assay. Data are presented as cell number relative to NK cells-free controls, mean + SE values for triplicate samples.

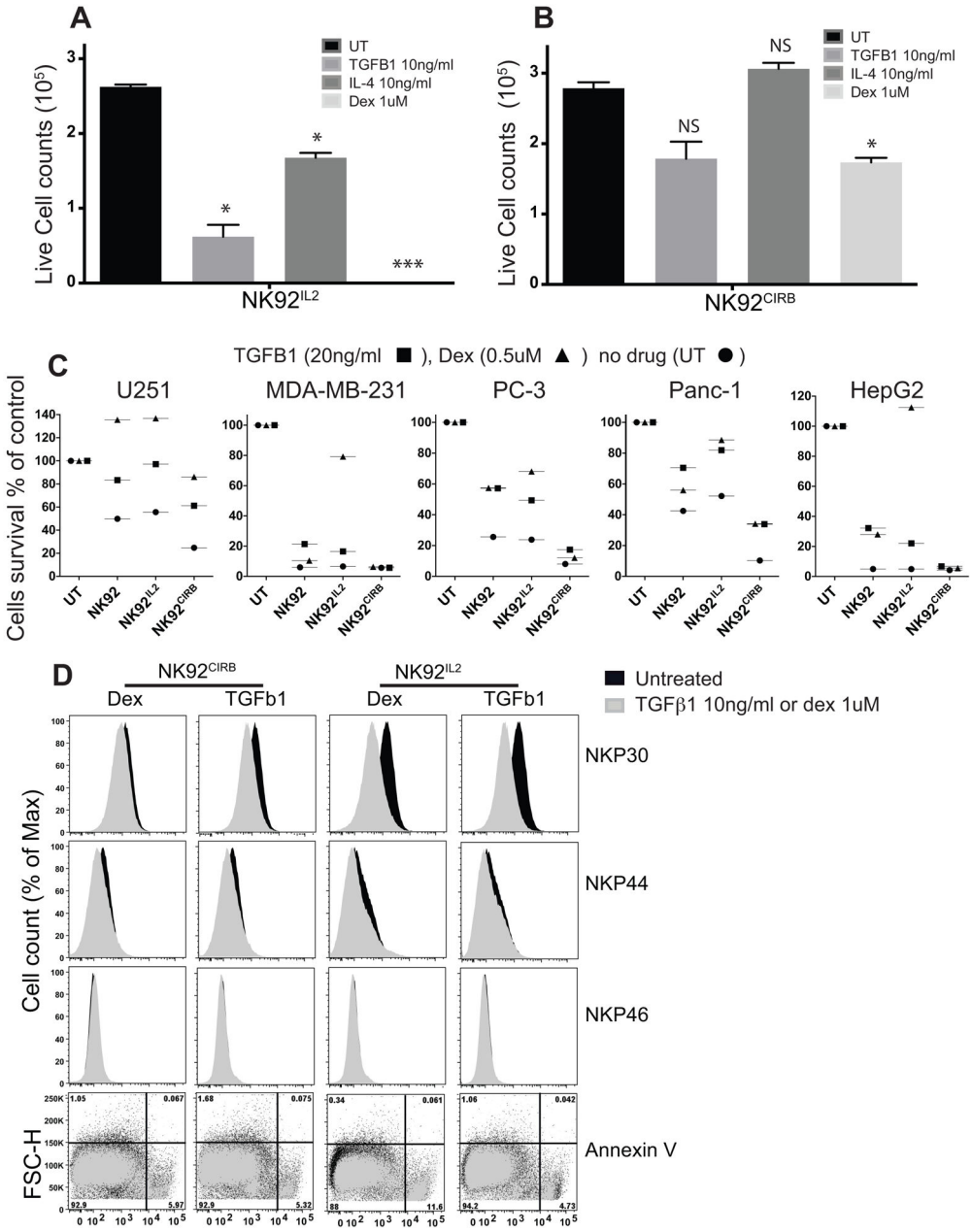

Figure 3.

Impact of TGFβ1, IL4 and Dexamethasone on NK cells. **A**, 64×10^3 $NK92^{IL2}$ and **B**, $NK92^{CIRB}$ cells were plated with TGFβ1 (10ng/ml), IL4 (10ng/ml), or Dex (1uM) for 6 days of growth. Viable cells were counted using Trypan blue exclusion assay. Data are presented as live cell count (10^5 cells/ml), mean + SE values for triplicate samples. **C**, NK92, $NK92^{IL2}$ and $NK92^{CIRB}$ cell lines exposed for 24 hours to TGFβ1 (20ng/ml■), Dex (0.5uM▲), or no drug (UT●). NK 92 cells were incubated with IL2 at 20IU/ml. Cancer cells (32×10^3 cells), were then added to NK cells at E/T ratio of 2:1, then incubated for 4 days. Cancer cells viability was determined using a crystal violet extraction assay. Data are presented as mean percentage cell number relative to NK cells-free controls (UT). **D**,

Natural cytotoxicity receptors and AnnexinV expression in $NK92^{IL2}$ and $NK92^{CIRB}$ treated with dex1uM or TGFβ1 10ng/ml.

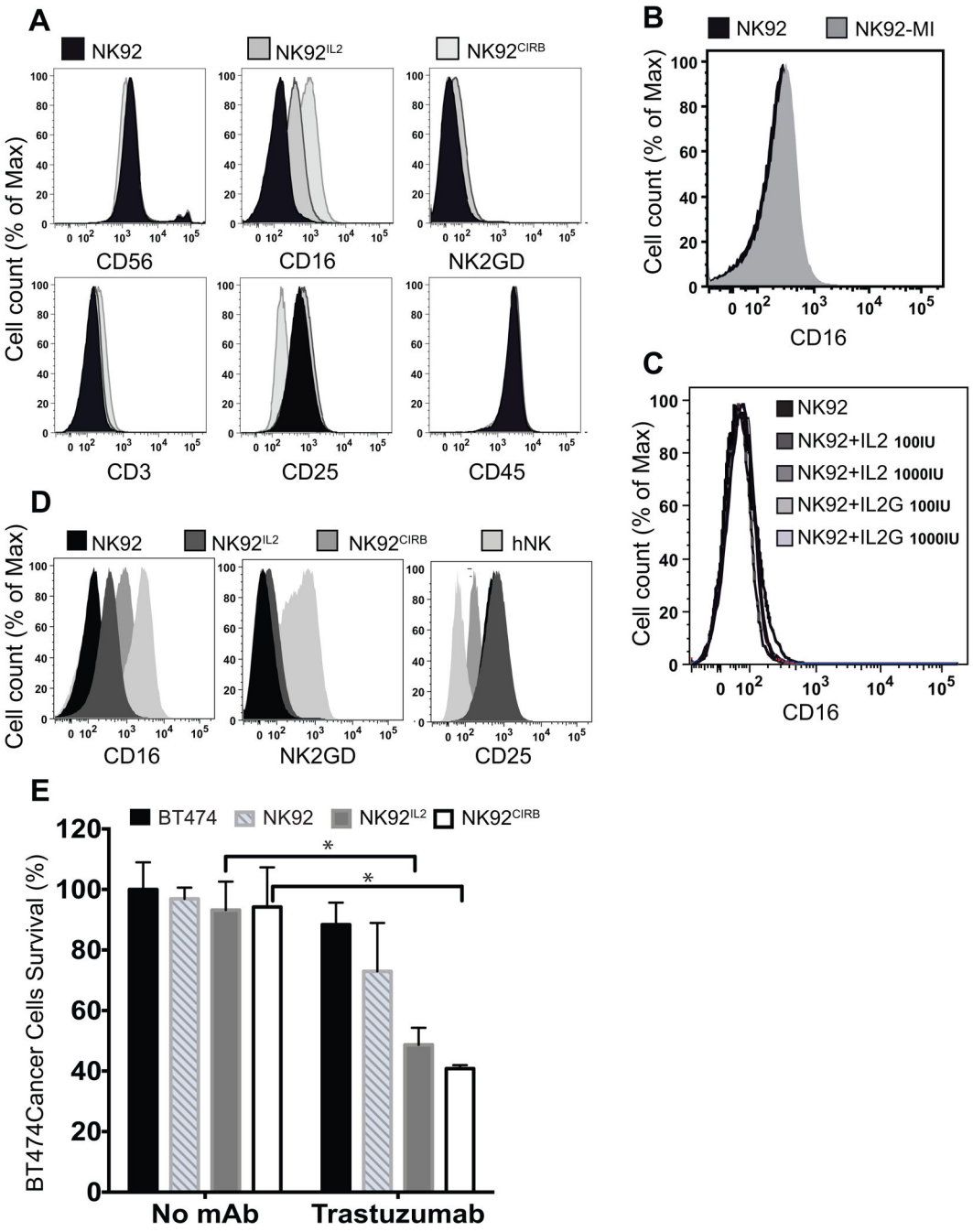

Figure 4.

NK92, NK92^{IL2} and NK92^{CIRB} cell lines phenotype. **A**, Flow cytometry shows the increased cell surface density of CD16 in NK92^{IL2} and NK92^{CIRB} and the low expression of CD25 in NK92^{CIRB}. **B**, Flow cytometry confirms the lack of expression of CD16 in NK92 and NK92-MI cell lines. **C**, shows the lack of expression of CD16 in NK92 activated with 100 or 1000IU/m of glycosylated (IL2G) and non glycosylated IL2. **D**, Human primary NK cells (hNK) phenotypic expression of NKG2D, CD25 and CD16 in comparison to NK92, NK92^{IL2} and NK92^{CIRB}. **E**, direct cytotoxicity and ADCC activity mediated by effector

NK92, NK92^{IL2} and NK92^{CIRB} cells against HER2 positive BT474 cell line at E/T ratio of 2:1 when incubated with Trastuzumab (1ug/ml). Data are presented as cell number percentage relative to NK cells-free controls, mean + SE values for triplicate samples. Statistical differences were determined by one-way Anova test ((*P<0.05).

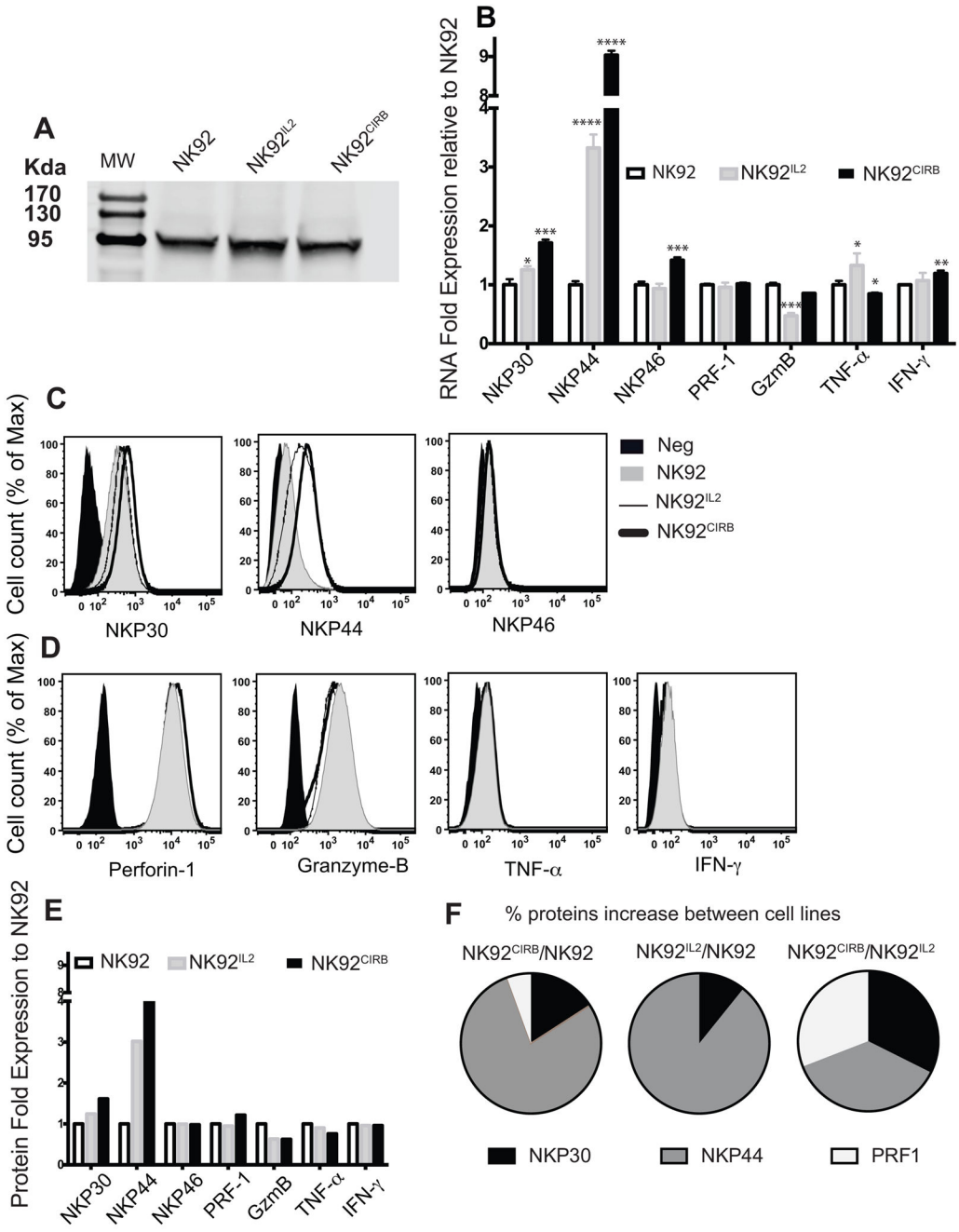

Figure 5.

Natural cytotoxity receptors and effectors in NK cell lines. **A**, Stat 5 phosphorylation is equivalent in NK92 and NK92^{CIRB} cells and higher by 17% in NK92^{IL2} as determined by ImageJ software. **B**, **Gene** expression profiles of NKP30, NKP44, NKP46, Granzyme-B, Perforin-1, TNF-α, and INF-γ in NK cells lines determined by qRT-PCR. Primers sequences in Supplementary Table S1. Results were analyzed using comparative C_T ($\Delta\Delta C_T$) method and are presented as RNA folds relative to NK92 after normalization to the GAPDH RNA content of each sample. Data are presented as mean + SE values for triplicate samples. Two tails t-test analysis was used to evaluate statistical differences. **C**, Surface expression by

flow cytometry of NKP30, NKP44, NKP46 and **D**, Granzyme-B, Perforin-1, TNF-α, and INF-γ. **E**, Statistical ∑Median values derived from data in (C) and (D) using FlowJo statistical module for 3×10^5 cells analyzed. **F**, Visualization of the percentage increase of markers expression between NK cell lines pairs.

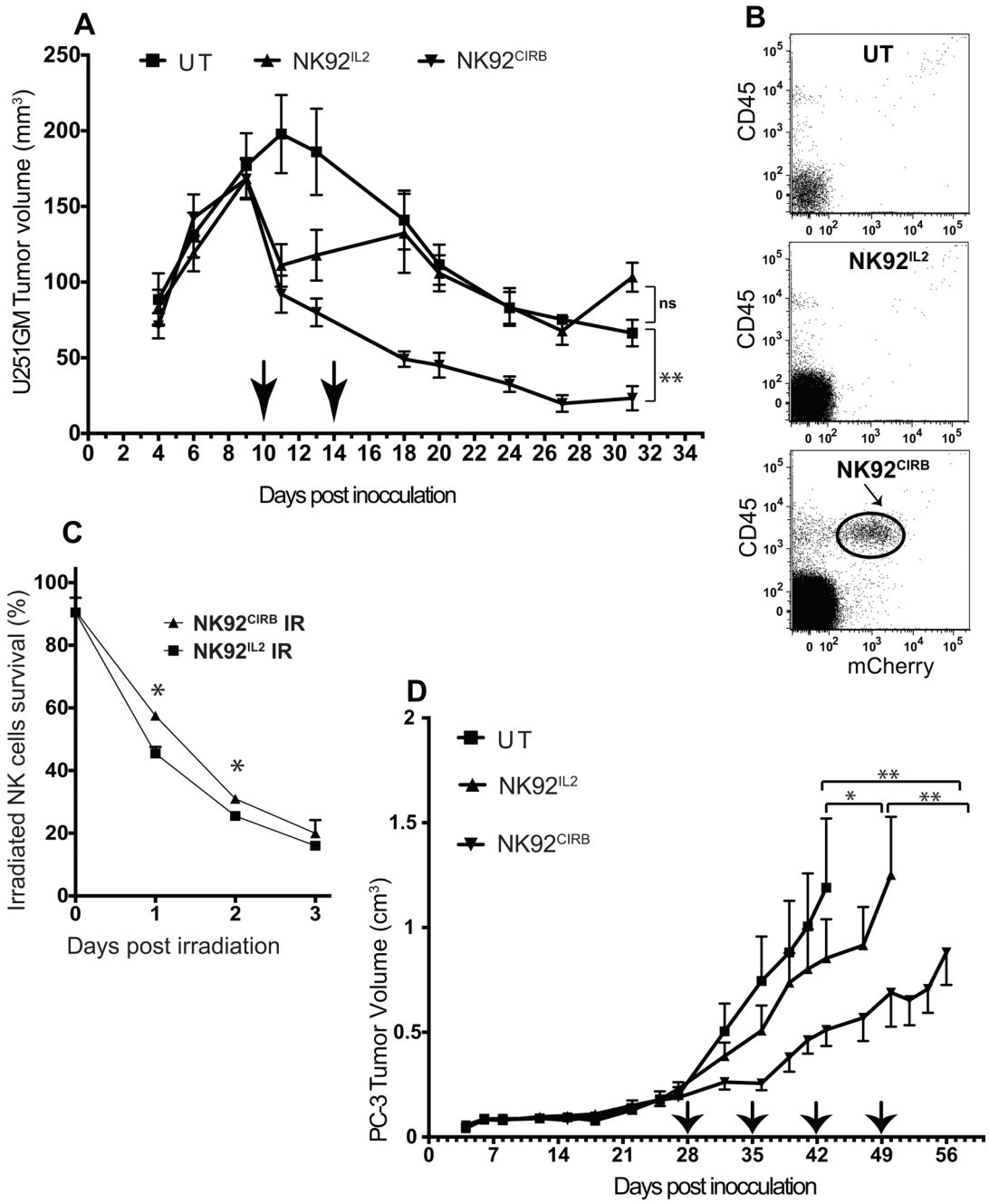

Figure 6.

NK92^{IL2} and NK92^{CIRB} cells evaluation *in vivo*. **A**, When U251 tumor volume reached ~160mm^3, non-irradiated NK92^{IL2} and NK92^{CIRB} cells (10^7 cells in 200ul per mouse) were injected into mice (arrows), via the tail vein. A second injection of non-irradiated NK cells (5×10^6 cells) was carried out 4 days later. Tumor sizes were monitored until 31 days post tumor implantation. **B**, 17 days after the last NK cells injection, animals were sacrificed and blood was collected from 3 animals in each group. Blood samples (0.5ml) were processed and analyzed by flow cytometry using human specific marker CD45 and the mCherry fluorescence marker, which is co-expressed with IL2 or CIRB in NK92^{IL2} and NK92^{CIRB},

respectively. $NK92^{CIRB}$ cells detected (circled). **C**, Cell survival of NK cells irradiated *in vitro* at 10Gy (0.83gy for 12 min) and then plated in complete NK92 media was determined using Trypan Blue exclusion every 24 hours. The survival advantage of $NK92^{CIRB}$ cells was statistically significant at days 1 and 2 (One-way Anova test *P<0.05). **D**, anti-tumor efficacy of irradiated $NK92^{IL2}$ and $NK92^{CIRB}$ cells *in vivo* against PC-3 tumors grown in 5 week-old male Nod/Scid mice. When tumor size reached ~200 mm^3, NK cells were irradiated with 500cGy were administered as four weekly injections of 15×10^6 cells in 200ul per mouse, via the tail vein (arrows). After the last $NK92^{CIRB}$ cells injection, a significant tumor growth delay of 17 days was recorded (**P<0.01), comparatively to the untreated group. $NK92^{IL2}$ treated group tumors produced a tumor delay of only 7 days (*P<0.05). Statistical differences were determined using One-way Anova test.

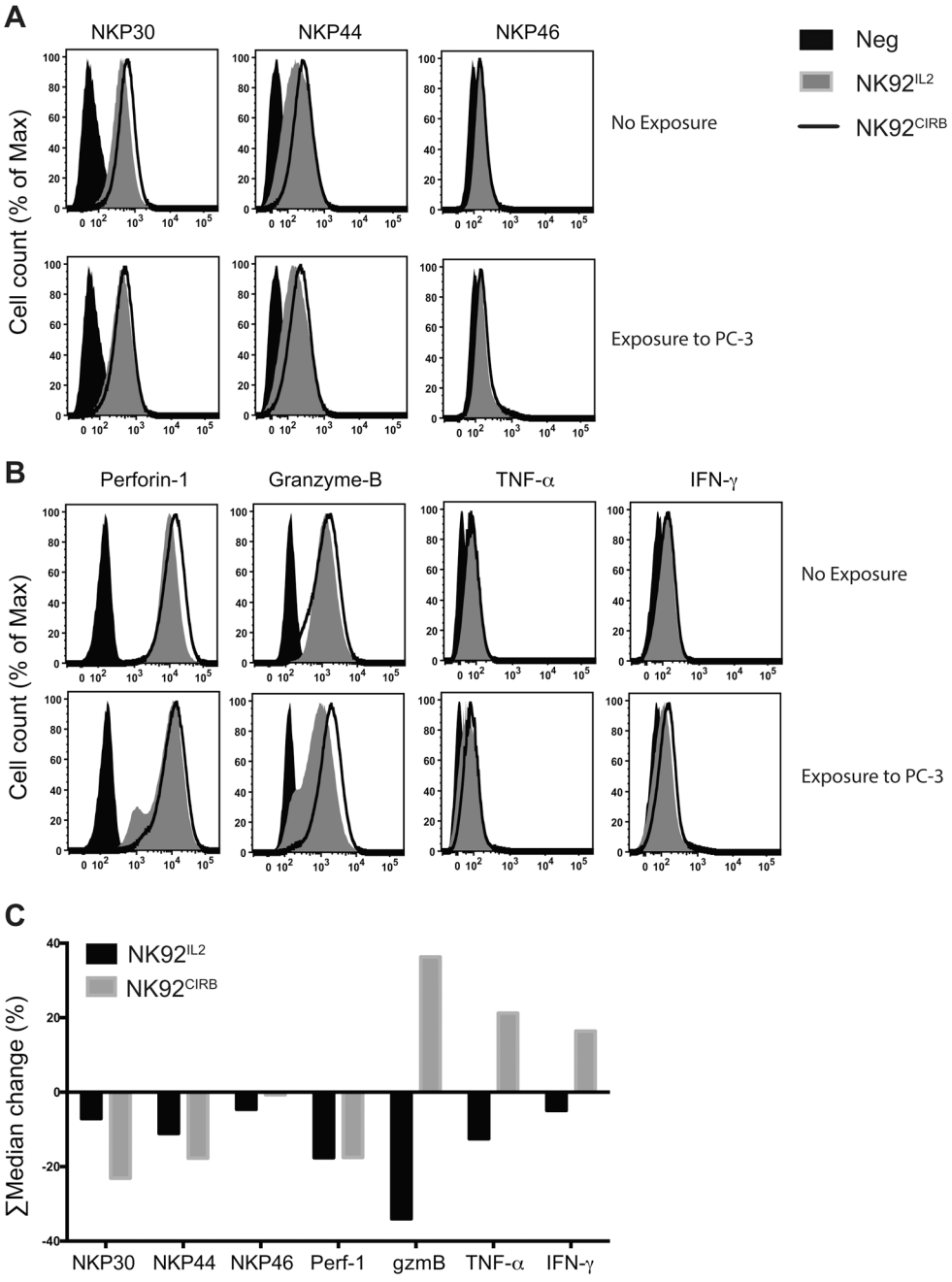

Figure 7.

NK92^{CIRB} and NK92^{IL2} cells activation by direct contact with PC-3 cancer cells. NK cells and PC-3 cells were co-cultured for a duration of 3 hours after which their expression profile of **A**, NKP30, NKP44, NKP46 and **B**, Perforin-1, Granzyme-B, TNF-α and IFN-γ, were compared to NK cells grown alone. **C**, ∑Median expression of histograms by FlowJo software of the data in A, B and supplementary Table S2. Data show the reduction in surface expression for NKP30, NKP44, and NKP46. In NK92^{IL2} Perforin-1, Granzyme-B, TNF-α and IFN-γ decreased suggesting release while they increased in NK92^{CIRB} (36%, 21% and 16%, respectively) implying replenishment of these effectors. After 3 hours of contact with

cancer cells, $NK92^{CIRB}$ cells still retained a distinct advantage by harboring all receptors and effectors in excess over $NK92^{IL2}$ (supplementary Table S2).